



Mathematical Models of Inverse Problems for Finding the Main Characteristics of Air Pollution Sources

Artur O. Zaporozhets · Vladyslav V. Khaidurov

Received: 14 September 2020 / Accepted: 15 November 2020 / Published online: 24 November 2020
© Springer Nature Switzerland AG 2020

Abstract The paper describes optimization of mathematical models for determining the main characteristics of the source of environmental pollution. A modification of the classical Newton's method for finding a numerical solution of the constructed mathematical models for identifying the parameters of an environmental pollutant has been developed. A modification of the classical Newton's method is obtained, which makes it possible to reduce the total number of calculations in the process of determining the main characteristics of the pollution source. A number of software-implemented computational experiments have been carried out for the model for determining the height of the pipe of the pollution source and the concentration of emissions on it, the model for determining the full location of the pipe of the pollution source and the concentration of emissions from the source. The possibility of complete localization of the pollution source in less than 40 measurement iterations using 1 post of the air pollution monitoring system has been established. The proposed method makes it possible to reduce by 3 times the number of simulation iterations for detecting a source of pollution in comparison with classical methods for solving inverse problems during monitoring of air pollution.

Keywords Turbulent diffusion equations · Atmospheric pollution · Inverse problem · Pollution source · Optimization model · Newton's method

1 Introduction

Environmental problems in the modern world occupy one of the priority places among the scientific community (Oves et al. 2018; Sładkowski 2020; Kapustnyk et al. 2019). This is primarily caused by a rapid increase in the average temperature on the planet (Assad et al. 2019; Lelieveld et al. 2016; Gasparrini et al. 2017; Caloiero 2017) due to an increase in greenhouse gases in the air (Meyer and Newman 2020; Van Vuuren et al. 2017; Zhu-Barker et al. 2017), which in turn is associated with the development of industry (Fraccascia and Giannoccaro 2019; Meng et al. 2017), an increase in the number of automobile (Kumar and Gupta 2016; Shiraki et al. 2020) and aviation (Hudda et al. 2020) transport, and other natural phenomena and anomalies (Herndon 2018). This also results in a general deterioration in the condition of atmospheric air.

Several approaches are now being used to reduce the amount of air pollutants:

1. Modernization of existing power equipment to improve its technical and economic characteristics (Zaporozhets 2019; Babak et al. 2020; Zaporozhets 2020; Dzikuć et al. 2020; Li et al. 2019);
2. Using of new types of fuel (biofuels, hydrogen, etc.) (Li et al. 2019; Tang et al. 2019; Devarajan et al.

A. O. Zaporozhets (✉) · V. V. Khaidurov
Institute of Engineering Thermophysics of NAS of Ukraine, Kyiv,
Ukraine
e-mail: a.o.zaporozhets@nas.gov.ua

- 2018; Slenkin and Geletukha 2007; Hasan and Rahman 2017);
3. Increasing the share of renewable energy sources (solar power, wind power, hydropower) (Hu et al. 2018; Liang et al. 2019; Hannan et al. 2019; Liddle and Sadorsky 2017; Pfeifer et al. 2019);
 4. Development of methods and means for the capture and recycling of pollutants from the air (Nematollahi and Carvalho 2019; Baker et al. 2017; Akram et al. 2016; Hua et al. 2017; Breyer et al. 2020; Rao et al. 2017);
 5. Increasing the amount of green spaces (Mader 2020; Dadvand and Nieuwenhuijsen 2019; Ren et al. 2017);
 6. Optimization of the urban environment to reduce the number of road transport (Figliozzi et al. 2020; Tajalli and Hajbabaie 2018; Penazzi et al. 2019), etc.

The problem of air pollution is very acute for many countries. For example, according to the World Health Organization, Ukraine ranks 1st place in the world in terms of the number of deaths from air pollution (Popov et al. 2020a). In other cities and regions of the world, the situation is also quite difficult (Di et al. 2017; Koengkan et al. 2020; Rappazzo et al. 2019).

To monitor ambient air quality, air pollution monitoring networks have become widespread (Idrees and Zheng 2020; Dhingra et al. 2019; Grace and Manju 2019; Guanochanga et al. 2019; Su 2018). Such networks can include both high-precision devices for the quantitative and qualitative analysis of air samples and relatively inexpensive sensor devices designed for indicative monitoring (Castell et al. 2017; Rai et al. 2017). Their main task is to signal the excess of certain concentrations of pollutants in the air (for example, $PM_{2.5}$, PM_{10} , O_3 , NO_x , SO_x , and CH_2O) (Zaporozhets et al. 2020; Yang and Wang 2017). But even a sufficiently large network of observation posts cannot always generate the necessary information. For this, methods of mathematical modeling are used.

Currently, a large number of models are used in practice to study the distribution of pollutants (Elperin et al. 2016; Larkin et al. 2017; Alimissis et al. 2018; Nasari et al. 2016). Such models solve both direct and inverse problems. The solution to the direct problem is reduced to creating a concentration

field according to the known characteristics of the pollution source. The solution of the inverse problem is reduced to finding the characteristics of the pollution source by the known values of the concentration of pollutants, determined at the posts of the air pollution monitoring network.

In the countries of Eastern Europe (Ukraine, Belarus, Russia, etc.), at the state level, either the OND-86 methodology or other methodologies close to the OND-86 is used (Sokolov 2017; Pavlovich et al. 2016). OND-86 allows to calculate the maximum possible distribution of emission concentrations under conditions of a weakly stable state of the atmosphere and averaged values over 20–30-min intervals, but does not take into account such factors as the stability class of the atmosphere and the type of the earth's surface (Popov et al. 2020b). This technique was applied to calculate the concentration of pollutants at a distance of up to 100 km from the emission source.

The methodology makes it possible to calculate the distribution of pollutants emitted into the atmosphere by single point, linear sources, and a group of sources, taking into account the influence of the terrain, to determine the limiting concentrations of pollutants in a two-meter layer above the earth's surface, as well as the vertical distribution of concentrations.

One of the main disadvantages of this methodology is the way of solving the inverse problem to determine the characteristics of the pollution source (Gochakov et al. 2018; Jafari et al. 2019). It directly provides for the presence of such a source (that is, the known location of the pollution source) that emits, and comes down to calculating the emission power M and the height of the pipe H from the value of the maximum surface concentration C_m . At the same time, it is impossible to find the location of the source of atmospheric air pollution (Kendler et al. 2020).

Thus, it can be concluded that the existing models for solving inverse problems in the study of the distribution of atmospheric air pollution need to be developed.

This article is devoted to the improvement of methods for modeling the distribution of pollutants for solving inverse problems, in particular, for localizing sources of air pollution according to the data of air pollution monitoring network.

2 Methods

2.1 General Approach

For modeling atmospheric pollution, the equation of turbulent diffusion was used, which has the form:

$$\frac{\partial C}{\partial t} + \sum_{i=1}^3 \left[U_i \frac{\partial C}{\partial X_i} \right] = \sum_{i=1}^3 \left[\frac{\partial}{\partial X_i} \left(K_i \frac{\partial C}{\partial X_i} \right) \right] - aC, \quad (1)$$

where t is the time parameter for the non-stationary model of the problem, described by this equation; X_i are spatial coordinates of the calculation area; U_i is the value of the average speed of movement of the pollution source along the spatial coordinates X_i ; K_i is the value of the exchange coefficient along the spatial coordinates; $i = 1, 2, 3$ are directions of the coordinate axes of spatial coordinates; a is the coefficient showing the change in concentration due to the transformation of the pollution source during the considered period of time; and C is the concentration of the pollution source during the entire calculation period.

Applying the Cartesian coordinate system, it was defined the axes X_1, X_2 , and X_3 through x, y , and z , respectively; speed $-U_1 = u, U_2 = v, U_3 = w$; and exchange coefficients $-K_1 = k_x, K_2 = k_y, K_3 = k_z$.

Therefore, Eq. (1) takes the following form:

$$\frac{\partial C}{\partial t} + u \frac{\partial C}{\partial x} + v \frac{\partial C}{\partial y} + w \frac{\partial C}{\partial z} = \frac{\partial}{\partial x} \left(k_x \frac{\partial C}{\partial x} \right) + \frac{\partial}{\partial y} \left(k_y \frac{\partial C}{\partial y} \right) + \frac{\partial}{\partial z} \left(k_z \frac{\partial C}{\partial z} \right) - aC. \quad (2)$$

In the process of solving real practical problems, the form of Eq. (2) can be significantly simplified. If the axis is oriented in the direction of the average wind speed, then $v = 0$.

The considered version of the model is some idealized, since it does not take into account the influence of other pollution sources and anthropogenic factors. This article discusses the possibility of localizing one pollution source with using one sensor. The inverse problems in the article are based on direct problems, which, in turn, are solved by both deterministic and stochastic methods. Such models effectively describe the distribution of pollutants over limited distances.

2.2 Setting Goals. Simulation of a Two-dimensional Case. Direct Problem

The equation is considered in the calculation area $\Omega = [0; 1]^2$:

$$\frac{\partial C}{\partial t} + u \frac{\partial C}{\partial x} + w \frac{\partial C}{\partial z} = \frac{\partial}{\partial x} \left(k_x \frac{\partial C}{\partial x} \right) + \frac{\partial}{\partial z} \left(k_z \frac{\partial C}{\partial z} \right), \quad (3)$$

where $u = 0.25; w = 0.03; k_x = k_z = 1; t = [0; 0.5]$.

The initial condition for (3) has the form:

$$C(x, z, 0)|_{(x,z) \in \Omega} = 0. \quad (4)$$

Condition (4) guarantees that at the initial moment of time the concentration of air pollutant is absent, that is, equal to zero.

The conditions at the boundary Γ of the calculation area in (3) are as follows:

$$\left(\frac{\partial C(x, z, t)}{\partial \vec{n}} \right) \Big|_{\Gamma} = 0, \quad (5)$$

where \vec{n} is the normal vector to the boundary of the calculation area Ω .

The internal condition at the source of pollution for (3) has the form:

$$C(x_{Src}, z_{Src}, t) = 1. \quad (6)$$

In Eq. (6), $(x_{Src}, z_{Src}) = (0.67; 0.32)$ are coordinates of the geometrical position of the pollution source. For monitoring the concentration in a fixed position, the point of the calculation area Ω was chosen, which receives data during the entire time period of the calculation, namely, for $t = [0; 0.5]$.

The data received by the sensor can be written as follows:

$$C_{DS} = C(x_S, z_S, t), t \in [0; 0.5], \quad (7)$$

where $(x_S, z_S) = (0.32; 0.83)$ are coordinates of the geometric position of the sensor.

The posed problem, described by Eqs. (3)–(6), modeled in the MATLAB 2019b application software package. The simulation results are shown in Fig. 1.

As a result of modeling the problem according to Eqs. (3)–(6), data for Eq. (7) is obtained. A graphical representation of the results of solving Eq. (7) is shown in Fig. 2.

So, the data from the sensor make it possible to solve a number of inverse problems (Golovnyia and Khaidurov 2017; Petrov et al. 2018; Adam and Branda

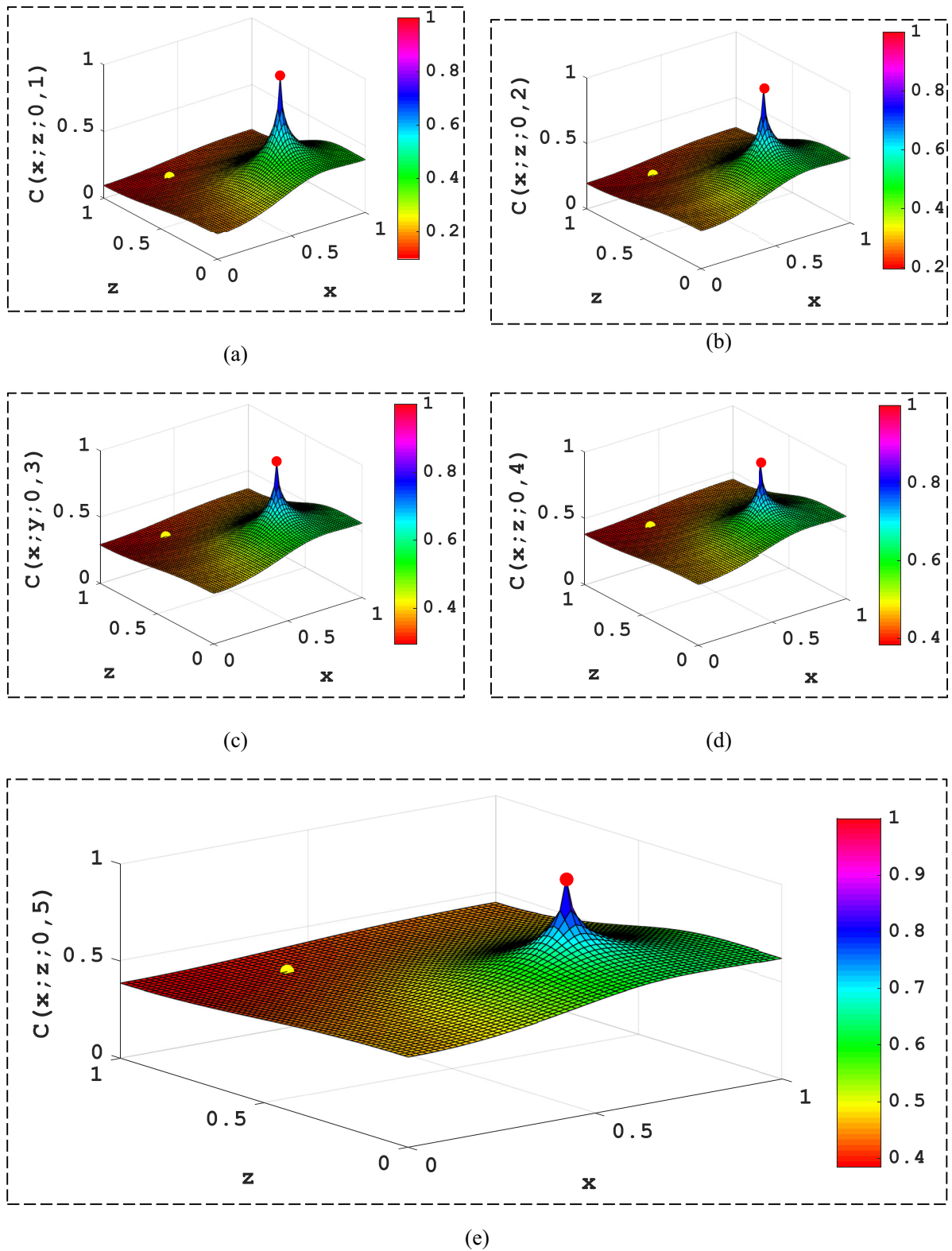


Fig. 1 Results of solving the problem by formulas (3)–(6) with a pollution source (red point) and a sensor (yellow point), which determines the pollutant’s concentration: **a–e** concentration distributions $C(x, z, t)$ at time points $t = 0.1; t = 0.2; t = 0.3; t = 0.4;$ and $t = 0.5$ respectively

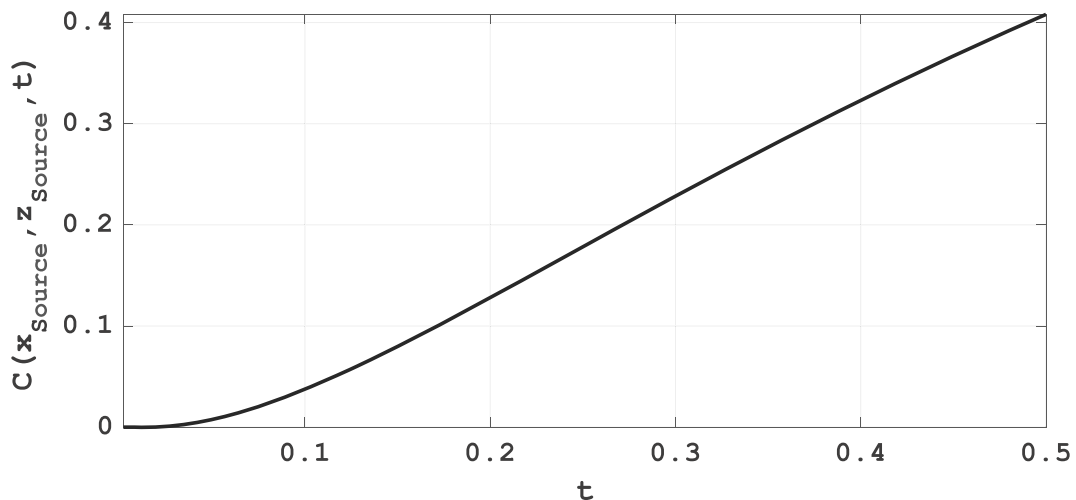


Fig. 2 The data obtained by the sensor, which is the result of solving Eqs. (3)–(6)

2016; Penenko et al. 2019), with the help of which it is possible to establish the position of the pollution source.

2.3 Simulation of a Two-dimensional Case. Inverse Problem Models

The solution of such problems in ecology can be solved using Eq. (7). According to the results of measurements in such problems, the characteristics of the pollution source are determined. Based on the data from the sensor, it is possible to construct the first mathematical model of the inverse problem based on the turbulent diffusion Eq. (3) is a model for determining the height of the pollution source and the concentration of emissions on it.

The second mathematical model of the inverse problem, based on the turbulent diffusion Eq. (3), is a model for determining the coordinates of the location of the pollution source pipe, its height and concentration of emissions, which it generates.

First Mathematical Model of the Inverse Problem The problem is posed in an optimization form. It is necessary to find the global minimum of a functional of the form:

$$J(z_{Src}, C_{Src}) = \int_{\tau_{beg}}^{\tau_{end}} (C_{DS}(C_{Src}(x_{Src}, z_{Src}), t) - C_{DS}(t))^2 dt, \tag{8}$$

where $C_{DS}(t)$ is data on the concentration of a pollutant in the air obtained by the sensor as a result of direct measurements, which is located in position (x_S, z_S) ;

$C_{DS}(C_{Src}(x_{Src}, z_{Src}), t)$ is data of the concentration of the pollutant on the sensor, obtained as a result of indirect measurements. This value depends on the position of the pollution source and the concentration C_{Src} that it generates.

The restriction on functional (8) is a turbulent diffusion equation of the form (3) with initial and boundary conditions (4) and (5), respectively. The value $C_{DS}(t)$ is the observation statistics and is set in a table form:

$$C_{DS}(t_i) = TableData_i, i = \overline{1, N}, \tag{9}$$

where N is the total number of observations. The data in Eq. (9) are given from Fig. 2.

The following mathematical model is a modification of the first model and consists in determining the geometric position of the pollution source, as well as the concentration of these emissions.

Second Mathematical Model of the Inverse Problem The problem is posed in an optimization form. It is necessary to find the global minimum of a functional of the form:

$$J(x_{Src}, z_{Src}, C_{Src}) = \int_{\tau_{beg}}^{\tau_{end}} (C_{DS}(C_{Src}(x_{Src}, z_{Src}), t) - C_{DS}(t))^2 dt, \tag{10}$$

where $C_{DS}(t)$ is the data on the concentration of a pollutant in the air obtained by the sensor as a result of direct measurements, which is located in position (x_S, z_S) ; $C_{DS}(C_{Src}(x_{Src}, z_{Src}), t)$ is data of the concentration of the pollutant on the sensor, obtained as a result of

indirect measurements. This value depends on the position of the pollution source and the concentration C_{Src} that it generates.

The restriction on functional (10) is a turbulent diffusion equation of the form (3) with initial and boundary conditions (4) and (5), respectively. The value $C_{DS}(t)$ is the observation statistics and is set by Eq. (9).

2.4 Methods for Solving Models of Inverse Problems

The process of solving inverse problems can be divided into several stages. Considering such problems from the point of view of the main aspects, obtaining optimal estimates and the content of the problems can be disclosed in several stages (Matsevityi et al. 2017).

- Stage I: solving the optimization problem, the optimal mathematical model is selected with the most convenient dependence of the input and output parameters.
- Stage II: choice of the form of setting the inverse problems and the ways to solve it.
- Stage III: selection of the optimal measurement vector, including smoothing and other forms of preliminary processing of experimental information.
- Stage IV: choice of a possible method or algorithm for solving, based on the type of mathematical model of the inverse problem, the degree of incorrectness of its formulation, computing facilities that are at the disposal of the researcher, and the software for them.
- Stage V: choice of the optimality criterion, the target functional, its norm, the method for finding the regularization parameters, the order of the stabilizing functional, and the method for minimizing the target functional.
- Stage VI: compilation of an optimal algorithm for solving the inverse problem, taking into account the chosen method, the optimality criterion, the required accuracy, and the shortest path to obtain stable solutions.
- Stage VII: selection of optimal computational procedures and implementation of the corresponding algorithm.
- Stage VIII: analysis of the solutions obtained, including preliminary processing of the results (approximation, smoothing, etc.).

The process of solving the inverse problem does not necessarily include all the listed stages or all the actions of each stage. It depends on the method used. Any method can be used at different stages, and during solving one problem, as a rule, several methods are used (Babak et al. 2019; Eremenko et al. 2020; Zaporozhets et al. 2018). In order to choose the optimal research method, it is necessary to have an idea of the whole variety of existing methods, which must be clearly systematized. There are various classifications of methods for solving the main classes of inverse problems.

Functionals of the forms (8) and (10) are minimized by solving a system of nonlinear equations. Let designate all unknown parameters of functionals (8) and (10) in the form of the vector $\vec{x} = (x_1, \dots, x_i, \dots, x_n)$. The system of equations has the form (Van Vuuren et al. 2017; Fraccascia and Giannoccaro 2019):

$$\left\{ \frac{\partial J}{\partial x_i} = 0 \right\}, i = \overline{1, N}, \quad (11)$$

where x_i are sought-for values of the parameters of functionals of the form (8), (10); N is the total number of parameters in the corresponding functionality. The number of unknown parameters in functional (8) is 2, and 3 in functional (10).

System (11) can be solved by Newton's method and its modifications (Schleicher and Stoll 2017; Ramos and Monteiro 2017).

Then, the optimization problem can be posed as follows. Among the numerous existing optimization methods of Newton's type, it is necessary to choose the most effective one for finding solutions to models of the posed inverse problems and to reduce the number of calls to the procedure for solving the direct problem in them.

Example. Let $f(\vec{x}) \rightarrow \min, x \in R^n$. First, it can be applied the steepest descent method to the unconstrained optimization problem. As the direction of descent, it can be chosen movement along the antigradient, for example, as (Lakhno et al. 2020):

$$\vec{x}^{(k+1)} = \vec{x}^{(k)} - h_k f' \left(\vec{x}^{(k)} \right), h_k > 0, k = 0, 1, 2, \dots$$

The problem consists in finding at each step such a value h_k that minimizes the function for a certain vector $\vec{x}^{(k)}$, and which is taken from the previous iteration number k . The search for such a value h_k can be implemented using any methods of one-dimensional

unconstrained optimization. The value of the parameter $h_k \in R^1$ is taken from the condition of the minimum of the function $f(\vec{x}^{(k)})$ in the direction of movement of the antigradient:

$$f\left(\vec{x}^{(k)} - h_k \cdot \nabla f\left(\vec{x}^{(k)}\right)\right) = \min f\left(\vec{x}^{(k)} - h \cdot \nabla f\left(\vec{x}^{(k)}\right)\right), h > 0.$$

So, using approximations to the initial condition, the sought-for value can be refined using the steepest descent method.

2.5 Modifications of the Classical Newton Method

Methods of this type replace the procedure for solving a nonlinear system of equations of the form $F_i(\vec{x}) = F_i(x_1, \dots, x_n) = 0, i = \overline{1, N}$ by a procedure for finding a solution to a sequence of systems of algebraic equations of the form:

$$\begin{pmatrix} \frac{\partial F_1}{\partial x_1}(\vec{x}^{(k)}) & \dots & \frac{\partial F_1}{\partial x_n}(\vec{x}^{(k)}) \\ \dots & \dots & \dots \\ \frac{\partial F_n}{\partial x_1}(\vec{x}^{(k)}) & \dots & \frac{\partial F_n}{\partial x_n}(\vec{x}^{(k)}) \end{pmatrix} \begin{pmatrix} x_1^{(k+1)} - x_1^{(k)} \\ \dots \\ x_n^{(k+1)} - x_n^{(k)} \end{pmatrix} = - \begin{pmatrix} F_1(\vec{x}^{(k)}) \\ \dots \\ F_n(\vec{x}^{(k)}) \end{pmatrix}. \tag{12}$$

Recall that it is necessary to find a solution to a system of the form (11), where the unknown parameters are the values of the required input parameters for functionals J of the forms (8) and (10). So, the matrix of system (12) will be the Hessian of the original system, that is, the matrix consisting of the second derivatives of the equations of the system:

$$H\left(\vec{x}^{(k)}\right) = \begin{pmatrix} \frac{\partial^2 J}{\partial x_1^2}\left(\vec{x}^{(k)}\right) & \dots & \frac{\partial^2 J}{\partial x_1 \partial x_n}\left(\vec{x}^{(k)}\right) \\ \dots & \dots & \dots \\ \frac{\partial^2 J}{\partial x_n \partial x_1}\left(\vec{x}^{(k)}\right) & \dots & \frac{\partial^2 J}{\partial x_n^2}\left(\vec{x}^{(k)}\right) \end{pmatrix}. \tag{13}$$

Since to calculate the Hessian in formula (13), the solution is differentiated with respect to the unknown parameters of the functionals, then, in the general case, it is simply impossible to find the derivative analytically in such problems. It must be found numerically using the truncated Taylor series. For the numerical search for the second derivative, it is necessary to have the value of the differentiated function at three points, and for the search for the mixed derivative—at four points.

Let us consider a simple case. Let it be required to solve a nonlinear equation of the form $F(x) = 0, x \in R^1$.

The classical Newton method, which solves this equation, is to apply the following relationship:

$$x_{k+1} = x_k - \left(F'(x_k)\right)^{-1} F(x_k). \tag{14}$$

The accuracy of method (14) can be improved by the following approach. Let it be required to solve a differential equation of the form $y' = f(x)$. Integrating both of its parts, we obtain the expression:

$$\begin{aligned} \left\{ \int_{x_k}^{x_{k+1}} y' dx = \int_{x_k}^{x_{k+1}} f(x) dx \right\} \\ = \left\{ y_{k+1} - y_k = \int_{x_k}^{x_{k+1}} f(x) dx \right\} \\ = \left\{ y_{k+1} = y_k + \int_{x_k}^{x_{k+1}} y'(x) dx \right\}. \end{aligned} \tag{15}$$

Obviously, the procedure for finding the integral is closely related to the accuracy of calculations. Using the right rectangles formula, Eq. (15) can be rewritten as follows:

$$\begin{aligned} \left\{ y_{k+1} = y_k + \int_{x_k}^{x_{k+1}} y'(x) dx \right\} = \left\{ y_{k+1} = y_k + h y'(x_k) \right\} = \\ = \left\{ y_{k+1} = y_k + (x_{k+1} - x_k) y'(x_k) \right\}. \end{aligned} \tag{16}$$

These transformations are reduced to the classical Newton's method if $y_{k+1} = 0$ in Eq. (16) and solving the equation with respect to x_{k+1} . It is known that the accuracy of one iterative step of the broken line method is $O(h^2)$. The classical Newton's method has a similar calculation accuracy. It is possible to increase the accuracy of one step during solving an equation using the predictor-corrector method. During applying the trapezoid method to find the integral, it will have:

$$\begin{aligned} \left\{ y_{k+1} = y_k + \int_{x_k}^{x_{k+1}} y'(x) dx \right\} = \left\{ y_{k+1} = y_k + 0.5h \left(y'(x_k) + y'(x_{k+1}) \right) \right\}, \\ \left\{ y_{k+1} = y_k + 0.5(x_{k+1} - x_k) \left(y'(x_k) + y'(x_{k+1}) \right) \right\}. \end{aligned} \tag{17}$$

In Eq. (17), the value $y'(x_{k+1})$ is unknown. It is being evaluated. Estimation is carried out using the polyline method as follows:

$$z = x_k - \beta \frac{y_k}{y'_k}, x_{k+1} = x_k - \frac{2y_k}{y'(x_k) + y'(z)}. \tag{18}$$

Table 1 Result of the convergence of Eq. (19) for an optimization problem with a functional of the form (8) (initial condition—zero vector, computational grid— 100×100)

Iteration number	Functional value (8)	Iteration number	Functional value (8)
1	$6.98,748 \cdot 10^{-1}$	16	$1.19674 \cdot 10^{-11}$
2	$1.46151 \cdot 10^{-1}$	17	$2.23452 \cdot 10^{-12}$
3	$2.89458 \cdot 10^{-2}$	18	$1.45486 \cdot 10^{-12}$
4	$6.25600 \cdot 10^{-3}$	19	$7.83028 \cdot 10^{-13}$
5	$1.23779 \cdot 10^{-3}$	20	$5.04763 \cdot 10^{-13}$
6	$2.33252 \cdot 10^{-4}$	21	$2.09415 \cdot 10^{-13}$
7	$4.96087 \cdot 10^{-5}$	22	$1.07125 \cdot 10^{-13}$
8	$9.44009 \cdot 10^{-6}$	23	$5.31579 \cdot 10^{-14}$
9	$1.91068 \cdot 10^{-6}$	24	$3.02859 \cdot 10^{-14}$
10	$3.63544 \cdot 10^{-7}$	25	$1.32068 \cdot 10^{-14}$
11	$7.07624 \cdot 10^{-8}$	26	$6.19477 \cdot 10^{-15}$
12	$1.47211 \cdot 10^{-8}$	27	$3.11823 \cdot 10^{-15}$
13	$3.00475 \cdot 10^{-9}$	28	$1.93539 \cdot 10^{-15}$
14	$5.48991 \cdot 10^{-10}$	29	$1.24313 \cdot 10^{-15}$
15	$1.09199 \cdot 10^{-10}$	30	$6.09122 \cdot 10^{-16}$

The parameter β can be taken equal to one. To speed up computations by reducing their total number, this

parameter can be searched using the steepest descent method at each iteration in Eq. (18).

Table 2 Result of the convergence of Eq. (19) for an optimization problem with a functional of the form (10) (initial condition—zero vector, computational grid— 100×100)

Iteration number	Functional value (8)	Iteration number	Functional value (8)
1	$9.25455 \cdot 10^{-1}$	20	$1.65711 \cdot 10^{-10}$
2	$2.38026 \cdot 10^{-1}$	21	$4.39884 \cdot 10^{-11}$
3	$7.85797 \cdot 10^{-2}$	22	$2.49719 \cdot 10^{-11}$
4	$2.28861 \cdot 10^{-2}$	23	$1.40827 \cdot 10^{-11}$
5	$6.99729 \cdot 10^{-3}$	24	$8.24481 \cdot 10^{-12}$
6	$2.60540 \cdot 10^{-3}$	25	$5.04120 \cdot 10^{-12}$
7	$1.02890 \cdot 10^{-3}$	26	$2.69363 \cdot 10^{-12}$
8	$3.35036 \cdot 10^{-4}$	27	$1.51376 \cdot 10^{-12}$
9	$1.22709 \cdot 10^{-4}$	28	$6.64779 \cdot 10^{-13}$
10	$3.80843 \cdot 10^{-5}$	29	$2.77332 \cdot 10^{-13}$
11	$1.33915 \cdot 10^{-5}$	30	$1.40636 \cdot 10^{-13}$
12	$4.05652 \cdot 10^{-6}$	31	$6.63584 \cdot 10^{-14}$
13	$1.44117 \cdot 10^{-6}$	32	$3.69366 \cdot 10^{-14}$
14	$4.43006 \cdot 10^{-7}$	33	$2.37507 \cdot 10^{-14}$
15	$1.60355 \cdot 10^{-7}$	34	$1.41103 \cdot 10^{-14}$
16	$5.69662 \cdot 10^{-8}$	35	$6.37278 \cdot 10^{-15}$
17	$1.66918 \cdot 10^{-8}$	36	$2.71298 \cdot 10^{-15}$
18	$5.14263 \cdot 10^{-9}$	37	$1.16343 \cdot 10^{-15}$
19	$1.51835 \cdot 10^{-9}$	38	$5.04624 \cdot 10^{-16}$

Table 3 Comparative analysis of the efficiency of the obtained method in comparison with the classical Newton’s method

Method functional	Method (19) for a constant value $\beta = 1$	Method (19) for β obtained by the steepest descent method	Classical Newton’s method
Functional (8)	65%	29%	100%
Functional (10)	73%	31%	100%

So, the finally obtained optimization method for the considered functionals is as follows:

$$\begin{aligned} \vec{z} &= \vec{x}^{(k)} - \beta H^{-1} \left(\vec{x}^{(k)} \right) J \left(\vec{x}^{(k)} \right), \vec{x}^{(k+1)} \\ &= \vec{x}^{(k)} - 2 \left(H \left(\vec{x}^{(k)} \right) + H \left(\vec{z} \right) \right)^{-1} J \left(\vec{x}^{(k)} \right), \end{aligned} \tag{19}$$

where k is the iteration number of the optimization method; z is the intermediate values of unknown obtained parameters; $\vec{x}^{(k)}, \vec{x}^{(k+1)}$ are values of the unknown parameters obtained in the mathematical models for identifying the characteristics of the pollution source at iterations k and $(k + 1)$, respectively; $J(\cdot)$ is the vector of derivatives of the functional; and $H(\cdot)$ is the Hesse matrix (Hessian).

3 Results

The convergence of the method is described by Eq. (19) for the task of minimizing functional (8) with constraints in the form of Eqs. (3)–(5), and (9) is shown in Table 1. The number of iterations is 30. The problem was solved by the finite difference method on different grids, which have dimensions: $40 \times 40, 50 \times 50, 60 \times 60, 80 \times 80$, and 100×100 design nodes.

In the course of solving the problem, an approximate solution was obtained $(\tilde{z}_{Source}, C_{Source}) = (0.3192348764; 0.9946455187)$.

The resulting optimization method gives a more accurate result in contrast to the classical Newton method. After 30 iterations, the value of computational error of classical Newton method is $6.42 \cdot 10^{-6}$.

The convergence of the method described by Eq. (19) for the problem of minimizing functional (18) with constraints in the form of Eqs. (3)–(5), and (9) is shown

in Table 2. The number of iterations is 38. The problem was solved by the finite difference method on different grids, which have dimensions: $40 \times 40, 50 \times 50, 60 \times 60, 80 \times 80$, and 100×100 design nodes.

The resulting optimization method also gives a more accurate result in contrast to the classical Newton method. After 38 iterations, the value of computational error of classical Newton method is $1.55 \cdot 10^{-7}$.

The values in Tables 1 and 2 are given for the coefficient $\beta = 1$.

Table 3 contains a comparison of the results of the obtained method with the classical Newton’s method, as well as taking into account the steepest descent method to determine the optimal value of the β parameter.

The calculation accuracy for all computational experiments was set equal to 10^{-15} .

In the course of solving the problem, an approximate solution was obtained: $(\tilde{x}_{Source}, \tilde{z}_{Source}, \tilde{C}_{Source}) = (0.6201465184894 ; 0.3124693487; 0.9954751464)$.

4 Conclusions

The proposed model is a special case of atmospheric air pollution using 1 source of pollution with 1 post of the monitoring system. The resulting models can be modified to account for several different pollution sources. The total number of calculations in such models is directly proportional to the number of pollution sources and the number of equations describing the process, which is directly considered. It should be noted that the obtained modifications of the classical Newton method have a number of advantages. First, the total number of calculations for obtaining solutions to the problems posed has been reduced by more than 3 times for two different functionalities. Secondly, the method is much more stable than the classical one due to the selection of the optimal parameter, which is used directly both for decreasing and for obtaining stable solutions at each iteration of the method.

During numerically realizing mathematical models, which are based on inverse problems, it must be taken into account the fact that the amount of computation can be very large. Thus, to obtain a numerical solution to inverse problems in the optimization formulation, it is necessary to solve multiple direct problems that are related to one inverse problem. Despite the fact that stochastic methods do not require information about

the objective function, such as differentiability and local extrema, they can increase the number of calls to the procedure for solving the direct problem, and therefore the total number of calculations. If the objective function has local extrema, then it is advisable to use a combination of the obtained deterministic method and stochastic optimization methods in the complex.

Acknowledgments The project presented in this article is supported by «Development of a system for monitoring the level of harmful emissions of TPP and diagnosing the equipment of power plants using renewable energy sources on the basis of Smart Grid with their collaboration» (2019–2021, 0119U101859), which is financed by National Science of Ukraine, and «Development of a system for monitoring micro climatic parameters and the air pollution of the ecosystems the Northern Black Sea Coast (2019–2021, 0119U100550), which is financed by the Ukrainian Ministry of Education.

References

- Adam, L., & Branda, M. (2016). Sparse optimization for inverse problems in atmospheric modelling. *Environmental Modelling & Software*, *79*, 256–266. <https://doi.org/10.1016/j.envsoft.2016.02.002>.
- Akram, M., Ali, U., Best, T., Blakey, S., Finney, K. N., & Pourkashanian, M. (2016). Performance evaluation of PACT Pilot-plant for CO₂ capture from gas turbines with Exhaust Gas Recycle. *International Journal of Greenhouse Gas Control*, *47*, 137–150. <https://doi.org/10.1016/j.ijggc.2016.01.047>.
- Alimissis, A., Philippopoulos, K., Tzanis, C. G., & Deligiorgi, D. (2018). Spatial estimation of urban air pollution with the use of artificial neural network models. *Atmospheric Environment*, *191*, 205–213. <https://doi.org/10.1016/j.atmosenv.2018.07.058>.
- Assad, E. D., Ribeiro, R. R. R., & Nakai, A. M. (2019). Assessments and how an increase in temperature may have an impact on agriculture in Brazil and mapping of the current and future situation. In C. Nobre, J. Marengo, & W. Soares (Eds.), *Climate change risks in Brazil* (pp. 31–65). Cham: Springer. https://doi.org/10.1007/978-3-319-92881-4_3.
- Babak, V., Eremenko, V., & Zaporozhets, A. (2019). Research of diagnostic parameters of composite materials using Johnson distribution. *Int. J. Comput.*, *18*(4), 483–494.
- Babak, V. P., Babak, S. V., Myslovych, M. V., Zaporozhets, A. O., & Zvaritch, V. M. (2020). Technical provision of diagnostic systems. In *Diagnostic systems for energy equipments. Studies in Systems, Decision and Control* (Vol. 281, pp. 91–133). Cham: Springer. https://doi.org/10.1007/978-3-030-44443-3_4.
- Baker, R. W., Freeman, B., Kniep, J., Wei, X., & Merkel, T. (2017). CO₂ capture from natural gas power plants using selective exhaust gas recycle membrane designs. *International Journal of Greenhouse Gas Control*, *66*, 35–47. <https://doi.org/10.1016/j.ijggc.2017.08.016>.
- Breyer, C., Fasihi, M., & Aghahosseini, A. (2020). Carbon dioxide direct air capture for effective climate change mitigation based on renewable electricity: a new type of energy system sector coupling. *Mitigation and Adaptation Strategies for Global Change*, *25*(1), 43–65. <https://doi.org/10.1007/s11027-019-9847-y>.
- Caloiero, T. (2017). Trend of monthly temperature and daily extreme temperature during 1951–2012 in New Zealand. *Theoretical and Applied Climatology*, *129*, 111–127. <https://doi.org/10.1007/s00704-016-1764-3>.
- Castell, N., Dauge, F. R., Schneider, P., Vogt, M., Lerner, U., Fishbain, B., et al. (2017). Can commercial low-cost sensor platforms contribute to air quality monitoring and exposure estimates? *Environment International*, *99*, 293–302. <https://doi.org/10.1016/j.envint.2016.12.007>.
- Dadvand, P., & Nieuwenhuijsen, M. (2019). Green space and health. In M. Nieuwenhuijsen & H. Khreis (Eds.), *Integrating human health into urban and transport planning* (pp. 409–423). Cham: Springer. https://doi.org/10.1007/978-3-319-74983-9_20.
- Devarajan, Y., Mahalingam, A., Munuswamy, D. B., et al. (2018). Emission and combustion profile study of unmodified research engine propelled with neat biofuels. *Environmental Science and Pollution Research*, *25*, 19643–19656. <https://doi.org/10.1007/s11356-018-2137-5>.
- Dhingra, S., Madda, R. B., Gandomi, A. H., Patan, R., & Daneshmand, M. (2019). Internet of Things mobile–air pollution monitoring system (IoT-Mobair). *IEEE Internet of Things Journal*, *6*(3), 5577–5584. <https://doi.org/10.1109/JIOT.2019.2903821>.
- Di, Q., Wang, Y., Zanobetti, A., Wang, Y., Koutrakis, P., Choirat, C., et al. (2017). Air pollution and mortality in the Medicare population. *New England Journal of Medicine*, *376*(26), 2513–2522. <https://doi.org/10.1056/NEJMoal702747>.
- Dzikuć, M., Kuryło, P., Dudziak, R., Szufa, S., Dzikuć, M., & Godzisz, K. (2020). Selected aspects of combustion optimization of coal in power plants. *Energies*, *13*(9), 2208. <https://doi.org/10.3390/en13092208>.
- Elperin, T., Fominykh, A., & Krasovtsov, B. (2016). Effect of raindrop size distribution on scavenging of aerosol particles from Gaussian air pollution plumes and puffs in turbulent atmosphere. *Process Safety and Environmental Protection*, *102*, 303–315. <https://doi.org/10.1016/j.psep.2016.04.001>.
- Eremenko, V., Zaporozhets, A., Babak, V., Isaienko, V., & Babikova, K. (2020). Using Hilbert transform in diagnostic of composite materials by impedance method. *Periodica Polytechnica Electrical Engineering and Computer Science*, *64*(4). <https://doi.org/10.3311/PPee.15066>.
- Figliozzi, M., Saenz, J., & Faulin, J. (2020). Minimization of urban freight distribution lifecycle CO₂e emissions: results from an optimization model and a real-world case study. *Transport Policy*, *86*, 60–68. <https://doi.org/10.1016/j.tranpol.2018.06.010>.
- Fracccasia, L., & Giannoccaro, I. (2019). Analyzing CO₂ emissions flows in the world economy using global emission chains and global emission trees. *Journal of Cleaner Production*, *234*, 1399–1420. <https://doi.org/10.1016/j.jclepro.2019.06.297>.

- Gasparrini, A., Guo, Y., Sera, F., Vicedo-Cabrera, A. M., Huber, V., Tong, S., et al. (2017). Projections of temperature-related excess mortality under climate change scenarios. *The Lancet Planetary Health*, 1(9), e360–e367. [https://doi.org/10.1016/S2542-5196\(17\)30156-0](https://doi.org/10.1016/S2542-5196(17)30156-0).
- Gochakov, A. V., Penenko, A. V., Antokhin, P. N., & Kolker, A. B. (2018). Air pollution modelling in urban environment based on a priori and reconstructed data. In *IOP Conference Series: Earth and Environmental Science* (Vol. 211, No. 1, p. 012050). IOP Publishing Ltd.. <https://doi.org/10.1088/1755-1315/211/1/012050>.
- Golovnya, B., & Khaidurov, V. (2017). Some high-speed methods for solving nonlinear inverse heat conduction problems. *Cherkasy University Bulletin: Applied Mathematics. Informatics.*, 1–2, 71–90.
- Grace, R. K., & Manju, S. (2019). A comprehensive review of wireless sensor networks based air pollution monitoring systems. *Wireless Personal Communications*, 108(4), 2499–2515. <https://doi.org/10.1007/s11277-019-06535-3>.
- Guanochanga, B., et al. (2019). Real-time air pollution monitoring systems using wireless sensor networks connected in a cloud-computing, wrapped up web services. In K. Arai, R. Bhatia, & S. Kapoor (Eds.), *Proceedings of the Future Technologies Conference (FTC) 2018. FTC 2018. Advances in intelligent systems and computing, vol 880* (pp. 171–184). Cham: Springer. https://doi.org/10.1007/978-3-030-02686-8_14.
- Hannan, M. A., Lipu, M. H., Ker, P. J., Begum, R. A., Agelidis, V. G., & Blaabjerg, F. (2019). Power electronics contribution to renewable energy conversion addressing emission reduction: applications, issues, and recommendations. *Applied Energy*, 251, 113404. <https://doi.org/10.1016/j.apenergy.2019.113404>.
- Hasan, M. M., & Rahman, M. M. (2017). Performance and emission characteristics of biodiesel–diesel blend and environmental and economic impacts of biodiesel production: a review. *Renewable and Sustainable Energy Reviews*, 74, 938–948. <https://doi.org/10.1016/j.rser.2017.03.045>.
- Herndon, J. M. (2018). Air pollution, not greenhouse gases: the principal cause of global warming. *Journal of Geography, Environment Earth Science Intn*, 17(2), 1–8.
- Hu, H., Xie, N., Fang, D., & Zhang, X. (2018). The role of renewable energy consumption and commercial services trade in carbon dioxide reduction: evidence from 25 developing countries. *Applied Energy*, 211, 1229–1244. <https://doi.org/10.1016/j.apenergy.2017.12.019>.
- Hua, T., Li, Y., Zhao, X., Yin, X., Yu, J., & Ding, B. (2017). Stable low resistance air filter under high humidity endowed by self-emission far-infrared for effective PM2.5 capture. *Composites Communications*, 6, 29–33. <https://doi.org/10.1016/j.coco.2017.08.003>.
- Hudda, N., Durant, L. W., Fruin, S. A., & Durant, J. L. (2020). Impacts of aviation emissions on near-airport residential air quality. *Environmental Science & Technology*, 54(14), 8580–8588. <https://doi.org/10.1021/acs.est.0c01859>.
- Idrees, Z., & Zheng, L. (2020). Low cost air pollution monitoring systems: a review of protocols and enabling technologies. *Journal of Industrial Information Integration*, 17, 100123. <https://doi.org/10.1016/j.jii.2019.100123>.
- Jafari, H., Babaei, A., & Banihashemi, S. (2019). A novel approach for solving an inverse reaction–diffusion–convection problem. *Journal of Optimization Theory and Applications*, 183(2), 688–704. <https://doi.org/10.1007/s10957-019-01576-x>.
- Kapustnyk, V. A., Zavhorodniy, I. V., Boeckmann, I., Litovchenko, O. L., & Lalymenko, O. S. (2019). Experience of international collaboration in solving actual medical and biological problems of occupational health and ecology. *Ukrainian Journal of Occupational Health*, 4(57), 58–67. <https://doi.org/10.33573/ujoh2018.04.058>.
- Kendler, S., Nebenzal, A., Gold, D., Reed, P. M., & Fishbain, B. (2020). The effects of air pollution sources/sensor array configurations on the likelihood of obtaining accurate source term estimations. *Atmospheric Environment*, 117754. <https://doi.org/10.1016/j.atmosenv.2020.117754>.
- Koengkan, M., Fuinhas, J. A., & Silva, N. (2020). Exploring the capacity of renewable energy consumption to reduce outdoor air pollution death rate in Latin America and the Caribbean region. *Environmental Science and Pollution Research*, 1–19. <https://doi.org/10.1007/s11356-020-10503-x>.
- Kumar, R., & Gupta, P. (2016). Air pollution control policies and regulations. In U. Kulshrestha & P. Saxena (Eds.), *Plant responses to air pollution* (pp. 133–149). Singapore: Springer. https://doi.org/10.1007/978-981-10-1201-3_12.
- Lakhno, V., Sagun, A., Khaidurov, V., & Panasko, E. (2020). Development of an intelligent subsystem operating system incidents forecasting. *Technology audit and production reserves*, 2(52), 35–39. <https://doi.org/10.15587/1729-4061.2018.131644>.
- Larkin, A., Geddes, J. A., Martin, R. V., Xiao, Q., Liu, Y., Marshall, J. D., et al. (2017). Global land use regression model for nitrogen dioxide air pollution. *Environmental Science & Technology*, 51(12), 6957–6964. <https://doi.org/10.1021/acs.est.7b01148>.
- Lelieveld, J., Proestos, Y., Hadjinicolaou, P., et al. (2016). Strongly increasing heat extremes in the Middle East and North Africa (MENA) in the 21st century. *Climatic Change*, 137, 245–260. <https://doi.org/10.1007/s10584-016-1665-6>.
- Li, S., Zhou, C., & Wang, S. (2019). Does modernization affect carbon dioxide emissions? A panel data analysis. *Science of the Total Environment*, 663, 426–435. <https://doi.org/10.1016/j.scitotenv.2019.01.373>.
- Liang, Y., Yu, B., & Wang, L. (2019). Costs and benefits of renewable energy development in China's power industry. *Renewable Energy*, 131, 700–712. <https://doi.org/10.1016/j.renene.2018.07.079>.
- Liddle, B., & Sadorsky, P. (2017). How much does increasing non-fossil fuels in electricity generation reduce carbon dioxide emissions? *Applied Energy*, 197, 212–221. <https://doi.org/10.1016/j.apenergy.2017.04.025>.
- Mader, S. (2020). Plant trees for the planet: the potential of forests for climate change mitigation and the major drivers of national forest area. *Mitigation and Adaptation Strategies for Global Change*, 25(4), 519–536. <https://doi.org/10.1007/s11027-019-09875-4>.
- Matsevityi, J. M., Kostikov, A. O., Safonov, N. A., & Ganchyn, V. V. (2017). To the solution of non-stationary nonlinear reverse problems of thermal conductivity. *Journal of Mechanical Engineering*, 20(4), 15–23.
- Meng, M., Jing, K., & Mander, S. (2017). Scenario analysis of CO2 emissions from China's electric power industry. *Journal of Cleaner Production*, 142, 3101–3108. <https://doi.org/10.1016/j.jclepro.2016.10.157>.

- Meyer, K., & Newman, P. (2020). A planetary quota for carbon dioxide. In *Planetary accounting* (pp. 121–136). Singapore: Springer. https://doi.org/10.1007/978-981-15-1443-2_8.
- Nasari, M. M., Szyszkowicz, M., Chen, H., Crouse, D., Turner, M. C., Jerrett, M., et al. (2016). A class of non-linear exposure-response models suitable for health impact assessment applicable to large cohort studies of ambient air pollution. *Air Quality, Atmosphere and Health*, 9(8), 961–972. <https://doi.org/10.1007/s11869-016-0398-z>.
- Nematollahi, M. H., & Carvalho, P. J. (2019). Green solvents for CO₂ capture. *Current Opinion in Green and Sustainable Chemistry*, 18, 25–30. <https://doi.org/10.1016/j.cogsc.2018.11.012>.
- Oves, M., Khan, M. Z., & Ismail, I. M. (Eds.). (2018). *Modern age environmental problems and their remediation*. Springer International Publishing. <https://doi.org/10.1007/978-3-319-64501-8>.
- Pavlovich, L. B., Osokina, A. A., Surzhikov, D. V., & Lupenko, V. G. (2016). Reducing environmental impact on the basis of risk calculations. *Coke and Chemistry*, 59(9), 353–361. <https://doi.org/10.3103/S1068364X16090076>.
- Penazzi, S., Accorsi, R., & Manzini, R. (2019). Planning low carbon urban-rural ecosystems: an integrated transport land-use model. *Journal of Cleaner Production*, 235, 96–111. <https://doi.org/10.1016/j.jclepro.2019.06.252>.
- Penenko, V. V., Penenko, A. V., Tsvetova, E. A., & Gochakov, A. V. (2019). Methods for studying the sensitivity of air quality models and inverse problems of geophysical hydrothermodynamics. *Journal of Applied Mechanics and Technical Physics*, 60(2), 392–399. <https://doi.org/10.1134/S0021894419020202>.
- Petrov, A., Chernyakov, Y., Steblyanko, P., Demichev, K., & Haydurov, V. (2018). Development of the method with enhanced accuracy for solving problems from the theory of thermo-pseudoelastic plasticity. *Eastern-European Journal of Enterprise Technologies*, 4/7(94), 25–33. <https://doi.org/10.15587/1729-4061.2018.131644>.
- Pfeifer, A., Krajačić, G., Ljubas, D., & Duić, N. (2019). Increasing the integration of solar photovoltaics in energy mix on the road to low emissions energy system—economic and environmental implications. *Renewable Energy*, 143, 1310–1317. <https://doi.org/10.1016/j.renene.2019.05.080>.
- Popov, O., Iatsyshyn, A., Kovach, V., Artemchuk, V., Kameneva, I., Taraduda, D., et al. (2020a). Risk assessment for the population of Kyiv, Ukraine as a result of atmospheric air pollution. *Journal of Health and Pollution*, 10(25), 200303. <https://doi.org/10.5696/2156-9614-10.25.200303>.
- Popov, O., Taraduda, D., Sobyna, V., Sokolov, D., Dement, M., & Pomaza-Ponomarenko, A. (2020b). Emergencies at potentially dangerous objects causing atmosphere pollution: peculiarities of chemically hazardous substances migration. In V. Babak, V. Isaenko, & A. Zaporozhets (Eds.), *Systems, decision and control in energy I. Studies in Systems, Decision and Control*, vol 298 (pp. 151–163). Cham: Springer. https://doi.org/10.1007/978-3-030-48583-2_10.
- Rai, A. C., Kumar, P., Pilla, F., Skouloudis, A. N., Di Sabatino, S., Ratti, C., et al. (2017). End-user perspective of low-cost sensors for outdoor air pollution monitoring. *Science of the Total Environment*, 607, 691–705. <https://doi.org/10.1016/j.scitotenv.2017.06.266>.
- Ramos, H., & Monteiro, M. T. T. (2017). A new approach based on the Newton's method to solve systems of nonlinear equations. *Journal of Computational and Applied Mathematics*, 318, 3–13. <https://doi.org/10.1016/j.cam.2016.12.019>.
- Rao, C., Gu, F., Zhao, P., Sharmin, N., Gu, H., & Fu, J. (2017). Capturing PM_{2.5} emissions from 3D printing via nanofiber-based air filter. *Scientific Reports*, 7(1), 1–10. <https://doi.org/10.1038/s41598-017-10995-7>.
- Rappazzo, K. M., Joodi, G., Hoffman, S. R., Pursell Jr., I. W., Mounsey, J. P., Cascio, W. E., & Simpson Jr., R. J. (2019). A case-crossover analysis of the relationship of air pollution with out-of-hospital sudden unexpected death in Wake County, North Carolina (2013–2015). *Science of the Total Environment*, 694, 133744. <https://doi.org/10.1016/j.scitotenv.2019.133744>.
- Ren, Y., Qu, Z., Du, Y., Xu, R., Ma, D., Yang, G., et al. (2017). Air quality and health effects of biogenic volatile organic compounds emissions from urban green spaces and the mitigation strategies. *Environmental Pollution*, 230, 849–861. <https://doi.org/10.1016/j.envpol.2017.06.049>.
- Schleicher, D., & Stoll, R. (2017). Newton's method in practice: finding all roots of polynomials of degree one million efficiently. *Theoretical Computer Science*, 681, 146–166. <https://doi.org/10.1016/j.tcs.2017.03.025>.
- Shiraki, H., Matsumoto, K. I., Shigetomi, Y., Ehara, T., Ochi, Y., & Ogawa, Y. (2020). Factors affecting CO₂ emissions from private automobiles in Japan: the impact of vehicle occupancy. *Applied Energy*, 259, 114196. <https://doi.org/10.1016/j.apenergy.2019.114196>.
- Stadkowski, A. (2020). *Ecology in transport: problems and solutions*. Springer. <https://doi.org/10.1007/978-3-030-42323-0>.
- Slenkin, M., & Geletukha, G. (2007). Development of ecologically friendly technology for gasification of municipal solid wastes. In J. W. Sheffield & C. Sheffield (Eds.), *Assessment of hydrogen energy for sustainable development. NATO Science for Peace and Security Series C: Environmental Security* (pp. 243–247). Dordrecht: Springer. https://doi.org/10.1007/978-1-4020-6442-5_20.
- Sokolov, A. K. (2017). Conditions for a partial summation of SO₂ and NO₂ hazardous effect in gas emission regulations. *Thermal Engineering*, 64(12), 931–934. <https://doi.org/10.1134/S0040601517120084>.
- Su, J. (2018). Portable and sensitive air pollution monitoring. Light, science & applications, 7. <https://doi.org/10.1038/s41377-018-0017-x>.
- Tajalli, M., & Hajbabaie, A. (2018). Distributed optimization and coordination algorithms for dynamic speed optimization of connected and autonomous vehicles in urban street networks. *Transportation research part C: emerging technologies*, 95, 497–515. <https://doi.org/10.1016/j.trc.2018.07.012>.
- Tang, L., Qu, J., Mi, Z., et al. (2019). Substantial emission reductions from Chinese power plants after the introduction of ultra-low emissions standards. *Nature Energy*, 4, 929–938. <https://doi.org/10.1038/s41560-019-0468-1>.
- Van Vuuren, D. P., Stehfest, E., Gernaat, D. E., Doelman, J. C., Van den Berg, M., Harmsen, M., et al. (2017). Energy, land-use and greenhouse gas emissions trajectories under a green growth paradigm. *Global Environmental Change*, 42, 237–250. <https://doi.org/10.1016/j.gloenvcha.2016.05.008>.
- Yang, Z., & Wang, J. (2017). A new air quality monitoring and early warning system: air quality assessment and air pollutant

- concentration prediction. *Environmental Research*, 158, 105–117. <https://doi.org/10.1016/j.envres.2017.06.002>.
- Zaporozhets, A. (2019). Analysis of control system of fuel combustion in boilers with oxygen sensor. *Periodica Polytechnica*, 63(4), 241–248. <https://doi.org/10.3311/PPme.12572>.
- Zaporozhets, A. (2020). Experimental research of a computer system for the control of the fuel combustion process. In *Control of fuel combustion in boilers. Studies in Systems, Decision and Control* (Vol. 287, pp. 89–123). Cham: Springer. https://doi.org/10.1007/978-3-030-46299-4_4.
- Zaporozhets, A. O., Redko, O. O., Babak, V. P., Eremenko, V. S., & Mokiyuchuk, V. M. (2018). Method of indirect measurement of oxygen concentration in the air. *Naukovyi Visnyk Natsionalnoho Hirnychoho Universytetu*, 5, 105–114. <https://doi.org/10.29202/nvngu/2018-5/14>.
- Zaporozhets, A., Babak, V., Isaienko, V., & Babikova, K. (2020). Analysis of the air pollution monitoring system in Ukraine. In V. Babak, V. Isaienko, & A. Zaporozhets (Eds.), *Systems, decision and control in energy I. Studies in Systems, Decision and Control*, vol 298 (pp. 85–110). Cham: Springer. https://doi.org/10.1007/978-3-030-48583-2_6.
- Zhu-Barker, X., Bailey, S. K., Burger, M., & Horwath, W. R. (2017). Greenhouse gas emissions from green waste composting windrow. *Waste Management*, 59, 70–79. <https://doi.org/10.1016/j.wasman.2016.10.004>.

Publisher's Note Springer Nature remains neutral with regard to jurisdictional claims in published maps and institutional affiliations.